

# Missing monopole strength of the Hoyle state in the inelastic $\alpha+^{12}\text{C}$ scattering<sup>\*</sup>

Dao T. Khoa<sup>\*</sup> and Do Cong Cuong

*Institute for Nuclear Science and Technique, VAEC, P.O. Box 5T-160, Nghia Do,  
Hanoi, Vietnam.*

---

## Abstract

Analyses of the inelastic  $\alpha+^{12}\text{C}$  scattering at medium energies have indicated that the strength of the Hoyle state (the isoscalar  $0_2^+$  excitation at 7.65 MeV in  $^{12}\text{C}$ ) seems to exhaust only 7 to 9% of the monopole energy weighted sum rule (EWSR), compared to about 15% of the EWSR extracted from inelastic electron scattering data. The full monopole transition strength predicted by realistic microscopic  $\alpha$ -cluster models of the Hoyle state can be shown to exhaust up to 22% of the EWSR. To explore the missing monopole strength in the inelastic  $\alpha+^{12}\text{C}$  scattering, we have performed a fully microscopic folding model analysis of the inelastic  $\alpha+^{12}\text{C}$  scattering at  $E_{\text{lab}} = 104$  to 240 MeV using the 3- $\alpha$  resonating group wave function of the Hoyle state obtained by Kamimura, and a complex density-dependent M3Y interaction newly parametrized based on the Brueckner Hartree Fock results for nuclear matter. Our folding model analysis has shown consistently that the missing monopole strength of the Hoyle state is not associated with the uncertainties in the analysis of the  $\alpha+^{12}\text{C}$  scattering, but is most likely due to the short lifetime and weakly bound structure of this state which significantly enhances absorption in the exit  $\alpha+^{12}\text{C}^*(0_2^+)$  channel.

*Key words:* Inelastic  $\alpha$ -scattering,  $0_2^+$  state in  $^{12}\text{C}$ , folding model analysis,  $E0$  transition

*PACS:* 24.10.Eq, 25.55.Ci, 27.20.+n

---

Given a vital role in the stellar synthesis of Carbon, the isoscalar  $0_2^+$  state at 7.65 MeV in  $^{12}\text{C}$  (known as the Hoyle state) has been studied over the years in numerous experiments. Although this state was clearly identified long ago in the inelastic  $\alpha+^{12}\text{C}$  scattering at medium energies [1,2,3,4] and inelastic electron scattering [5] as an isoscalar  $E0$  excitation, our knowledge about its

---

<sup>\*</sup> Research supported, in part, by Natural Science Council of Vietnam, EU Asia-Link Program CN/ASIA-LINK/008 (94791) and Vietnam Atomic Energy Commission (VAEC).

<sup>\*</sup> Corresponding author,

*Email address:* khoa@vaec.gov.vn (Dao T. Khoa).

unique structure is still far from complete [6]. Since the Hoyle state lies slightly above the  $\alpha$ -decay threshold of 7.27 MeV, its wave function should have a dominant  $\alpha$  cluster component. In fact, the Hoyle state has been well described in terms of three  $\alpha$  clusters by the Resonating Group Method (RGM) some thirty years ago [7,8]. Very interesting is the condensate scenario suggested recently [9,10] where the three  $\alpha$  clusters were shown to condense into the lowest ( $s$ -state) of their potential, and thus, forming a Bose-Einstein condensate (BEC). A more complicated structure of the Hoyle state was shown by the Fermionic Molecular Dynamics (FMD) calculation [11] where the BEC wave function is mixed also with the molecular  ${}^8\text{Be}+\alpha$  configuration. In general, to validate conclusion made in the structure calculation, the wave functions must be carefully tested in the study of nuclear reactions exciting the Hoyle state. In this aspect, the model wave functions of the Hoyle state [8,11,12] have been shown to give a reasonable description of the inelastic electron scattering data. The electric monopole transition moment

$$M(E0, 0_1^+ \rightarrow 0_2^+) = e\sqrt{4\pi} \int_0^\infty \rho_{0_1^+ \rightarrow 0_2^+}^{\text{proton}}(r) r^4 dr \quad (1)$$

predicted by the RGM [8], BEC [10] and FDM [11] calculations is around 6.62, 6.45 and 6.53  $e \text{ fm}^2$ , respectively, which are about 20% larger<sup>1</sup> than the experimental moment  $M(E0) \approx 5.37 \pm 0.22 e \text{ fm}^2$  deduced from the  $(e, e')$  data [5]. The inelastic electron scattering probes, however, only the charge transition density and it is necessary to study also inelastic hadron scattering which probes the nuclear transition density. Such experiments have been done, e.g., for inelastic  ${}^3,4\text{He}, {}^6\text{Li}+{}^{12}\text{C}$  scattering [13,14,15] and the data analyses, either in the distorted wave Born approximation (DWBA) or coupled-channel (CC) formalism, were performed using the collective model form factor (FF) for the Hoyle state. These analyses indicated that the observed monopole transition strength of the Hoyle state exhausts about 7 to 9% of the isoscalar monopole energy weighted sum rule (EWSR). In particular, the DWBA analysis of the inelastic  $\alpha+{}^{12}\text{C}$  data, measured recently at  $E_{\text{lab}} = 240 \text{ MeV}$  with high precision [15], has found that the Hoyle state exhausts  $7.6 \pm 0.9\%$  of the EWSR. We recall that the sum rule fraction  $S_0$  of a monopole excitation is determined [16] as

$$S_0 = E_x |M(IS0, 0_1^+ \rightarrow 0_2^+)|^2 / \left( \frac{2\hbar^2 A \langle r^2 \rangle}{m} \right), \quad (2)$$

where  $E_x, m$  and  $A$  are the excitation energy, nucleon mass and target mass number, respectively,  $\langle r^2 \rangle$  is the mean square radius and  $M(IS0, 0_1^+ \rightarrow 0_2^+)$

---

<sup>1</sup> a direct comparison of (1) with the observed  $M(E0)$  can be made if the small difference between the charge- and proton transition densities is neglected.

is the isoscalar monopole transition moment which is determined by the same Eq. (1) but using the nuclear transition density instead of the charge transition density. If we assume  $M(IS0, 0_1^+ \rightarrow 0_2^+) \approx 2M(E0, 0_1^+ \rightarrow 0_2^+)/e$  and take  $\langle r^2 \rangle \approx 5.78 \text{ fm}^2$  (estimated using the ground state density of  $^{12}\text{C}$  given by the RGM [8]), then we obtain  $S_0 \approx 22.8, 21.7$  and  $22.2\%$  of the EWSR from the RGM [8], BEC [10] and FDM [11] results, respectively, and  $S_0 \approx 15.0 \pm 1.3\%$  of the EWSR from the experimental monopole moment, in a perfect agreement with  $S_0$  value given in Ref. [5]. Given a good description of the  $(e, e')$  data by the cluster models [8,9,10,11], we conclude that the monopole strength of the Hoyle state should exhaust 15 to 20% of the EWSR and a puzzle remains why at least half of the monopole strength of the Hoyle state is missing in the inelastic  $\alpha+^{12}\text{C}$  scattering.

To investigate the missing monopole strength of the Hoyle state, we have performed a consistent folding model analysis of the inelastic  $\alpha+^{12}\text{C}$  scattering at  $E_{\text{lab}} = 104$  to  $240$  MeV using microscopic nuclear densities obtained from the 3- $\alpha$  RGM wave functions by Kamimura [8], and a new complex density-dependent M3Y interaction. Before discussing our results, we recall that the same RGM nuclear densities [8] were used in a number of folding model studies (see, e.g., Refs. [17,18,19,20,21]) of the inelastic  $\alpha+^{12}\text{C}$  scattering. Excepting the early work by Bauhoff [17] where a density independent Gaussian has been used as  $\alpha N$  interaction in the single-folding calculation, other studies mentioned here have used the well-known DDM3Y [22] interaction in the double-folding calculation of the  $\alpha+^{12}\text{C}$  potentials. Since the DDM3Y interaction is real, the imaginary parts of both the optical potential (OP) and inelastic FF were chosen phenomenologically in these studies. For example, in the CC analysis of the  $\alpha+^{12}\text{C}$  scattering by Ohkubo and Hirabayashi [18,19] the imaginary inelastic FF was neglected and parameters of the Woods-Saxon imaginary OP were adjusted separately for each exit channel to obtain a good CC fit to the measured cross sections. Although one could achieve a reasonable description of the inelastic  $\alpha+^{12}\text{C}$  scattering data in such a CC analysis, an arbitrary choice of the imaginary potentials makes it difficult to estimate accurately the absolute  $E0$  transition strength. Up to now, the  $E0$  strength of the Hoyle state has been deduced from the DWBA or CC analyses of the inelastic  $^3,^4\text{He}, ^6\text{Li}+^{12}\text{C}$  scattering [13,14,15] using the breathing mode (BM) model [16] for the nuclear transition density

$$\rho_{0_1^+ \rightarrow 0_2^+}(r) = -\beta \left[ 3\rho_0(r) + r \frac{d\rho_0(r)}{dr} \right], \quad (3)$$

where  $\rho_0(r)$  is the ground-state (g.s.) density of  $^{12}\text{C}$ . In this case,  $S_0 = [\beta/\beta_{\text{max}}]^2$ , where  $\beta_{\text{max}}$  is the deformation parameter required for a monopole excitation to exhaust 100% of the EWSR (see Eq. (3.5) in Ref. [23]). The inelastic scattering FF is then obtained by (double) folding the transition density (3) with the effective nucleon-nucleon ( $NN$ ) interaction and projec-

tile g.s. density [24,25]. In the  $\alpha$ -nucleus scattering, one also uses a simpler approach to (single) fold the density (3) with an appropriate  $\alpha$ -nucleon ( $\alpha N$ ) interaction [26]. In general, the (complex) strength of the  $\alpha N$  or  $NN$  interaction is first adjusted to the best optical model or CC description of elastic scattering and then is used without any further renormalization to calculate the inelastic FF. As a result, the only parameter in the inelastic channel is the deformation parameter  $\beta$  which must be determined from the best DWBA or CC fit to the inelastic scattering data. Since the dilute  $\alpha$ -clustered structure of the Hoyle state is different from a monopole compression mode, the use of the BM density (3) in the folding model calculation might be questionable. In addition, the uncertainties of the effective  $NN$  or  $\alpha N$  interaction and the optical potential (OP) in the entrance and exit channels could also cause some deviation in the description of inelastic cross section which results on the missing  $E0$  strength.

We note that the RGM wave functions by Kamimura [8] were proven to give consistently a realistic description of the shell-like structure of the ground state  $0_1^+$ , first excited  $2_1^+$  (4.44 MeV) and  $3_1^-$  (9.64 MeV) states, and the  $\alpha$ -clustered structure of the  $0_2^+$  (7.65 MeV) Hoyle state. For the latter, the RGM wave function has been shown [10,12] to be very close to the BEC wave function and both of them give, in fact, nearly the same description of the inelastic  $\alpha+^{12}\text{C}$  scattering [20]. Thus, the RGM nuclear densities is a very good choice for the present folding model study. Concerning the effective  $NN$  interaction, a density dependent version of the M3Y-Paris interaction (dubbed as CDM3Y6 interaction [24]) is the most often used in our folding calculations. The CDM3Y6 density dependent parameters were carefully adjusted in the Hartree-Fock (HF) calculation to reproduce the saturation properties of nuclear matter [24]. However, like the DDM3Y version, the CDM3Y6 interaction is *real* and can be used to predict the real OP and inelastic FF only. To avoid a phenomenological choice of the imaginary potentials like those used in earlier folding model studies [18,19,20,21] of the inelastic  $\alpha+^{12}\text{C}$  scattering, we have constructed in the present work a new *complex*, density dependent M3Y-Paris interaction. The parameters of the complex density dependence were calibrated against the Brueckner Hartree-Fock (BHF) results [27] for the nucleon OP in nuclear matter by Jeukenne, Lejeune and Mahaux (JLM) at each considered energy. Namely, the *isoscalar* complex nucleon OP in nuclear matter is determined from the HF matrix elements of the new density dependent  $NN$  interaction as

$$U_0(E, \rho) = \sum_{j \leq k_F} [\langle kj | u_D(E, \rho) | kj \rangle + \langle kj | u_{EX}(E, \rho) | jk \rangle]. \quad (4)$$

Here  $k_F = [1.5\pi^2\rho]^{1/3}$  and  $k$  is the momentum of the incident nucleon which must be determined self-consistently from  $U_0$  as  $k = \sqrt{2m[E - \text{Re } U_0(E, \rho)]/\hbar^2}$ .

We have used in Eq. (4) two different CDM3Y functionals [24] to construct separately the *real* and *imaginary* parts of the density dependence, so that the real and imaginary parts of the effective  $NN$  interaction  $u_{D(\text{EX})}$  are determined as

$$\text{Re}[u_{D(\text{EX})}] = F_V(E, \rho)v_{D(\text{EX})}(s), \quad \text{Im}[u_{D(\text{EX})}] = F_W(E, \rho)v_{D(\text{EX})}(s). \quad (5)$$

The radial direct and exchange interactions  $v_{D(\text{EX})}(s)$  were kept unchanged, as derived from the M3Y-Paris interaction [28], in terms of three Yukawas (see, e.g., Ref. [25,29]). The parameters of the *complex* density dependence  $F_{V(W)}(E, \rho)$  were adjusted iteratively until  $U_0(E, \rho)$  agrees closely with the tabulated JLM results at each energy [27] as shown in Fig. 1. More details on

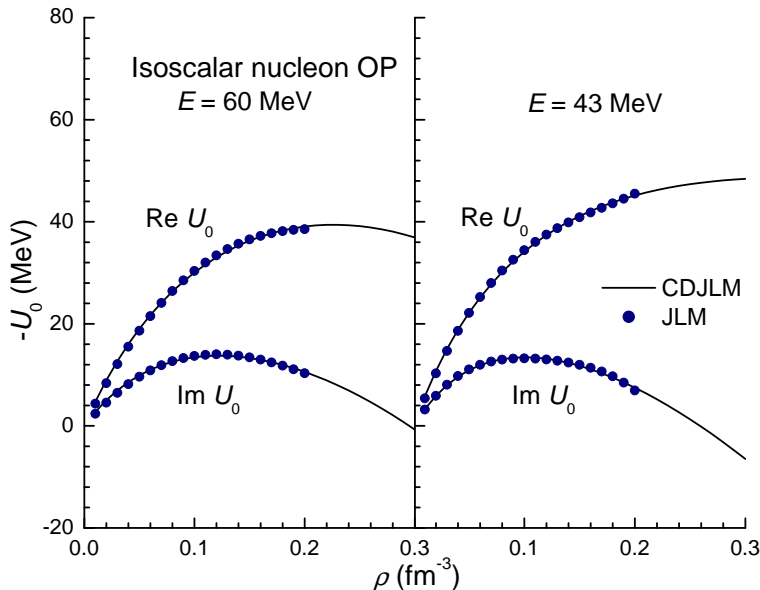


Fig. 1. Isoscalar optical potential  $U_0(E, \rho)$  of nucleon incident on nuclear matter at 43 and 60 MeV given by HF calculation (4) using the new CDJLM interaction (solid curves). The points are the microscopic BHF results made available up to nuclear matter density  $\rho = 0.2 \text{ fm}^{-3}$  by the JLM group [27]. This CDJLM interaction has been used in the present folding model study of the  $\alpha+^{12}\text{C}$  scattering at  $E_{\text{lab}} = 172.5$  and 240 MeV.

the new density dependent interaction, dubbed hereafter as CDJLM interaction, and the explicit parameters of  $F_{V(W)}(E, \rho)$  at different energies will be presented elsewhere. The CDJLM interaction was used to calculate the complex OP and inelastic FF for the microscopic DWBA and CC analyses of the elastic and inelastic  $\alpha+^{12}\text{C}$  scattering data at  $E_{\text{lab}} = 104$  [1,2], 139 [3], 172.5 [4], and 240 MeV [15]. The generalized double-folding method [25] was used to calculate the complex  $\alpha$ -nucleus potential as the following HF-type matrix

element of the CDJLM interaction (5)

$$U_{A \rightarrow A^*} = \sum_{i \in \alpha; j \in A, j' \in A^*} [\langle ij' | u_D | ij \rangle + \langle ij' | u_{EX} | ji \rangle], \quad (6)$$

where  $A$  and  $A^*$  are states of the target in the entrance- and exit channel of the  $\alpha$ -nucleus scattering, respectively. Thus, Eq. (6) gives the elastic (diagonal) OP if  $A^* = A$  and inelastic (transition) FF if otherwise. A more accurate local density approximation suggested in Ref. [30] has been used for the exchange term in Eq. (6). The dynamic change in the density dependence  $F_{V(W)}(\rho)$  caused by the inelastic  $\alpha + {}^{12}\text{C}$  scattering [25,31] is taken into account properly. All the DWBA and CC calculations have been performed using the code ECIS97 written by Raynal [32].

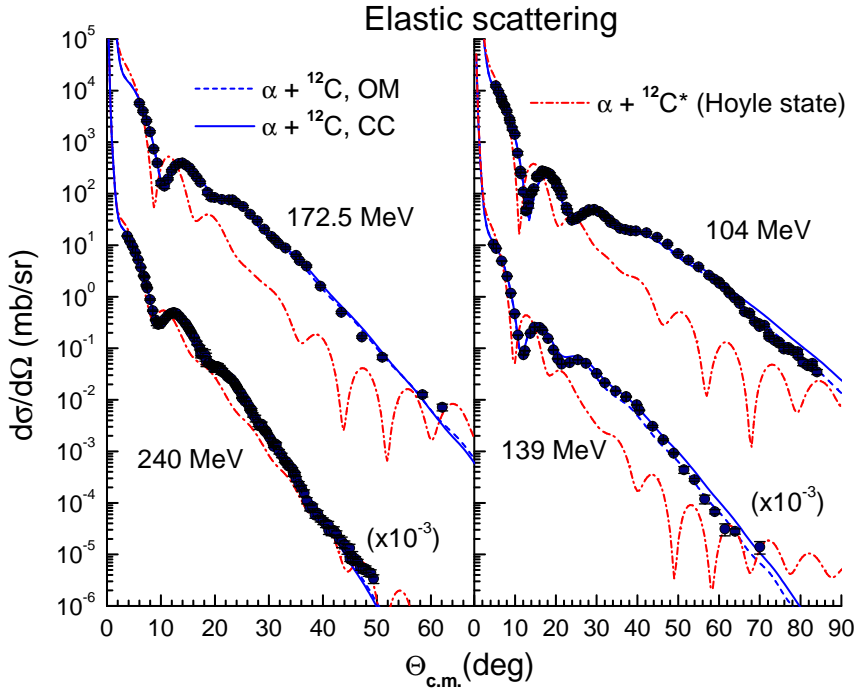


Fig. 2. Elastic  $\alpha + {}^{12}\text{C}$  scattering data measured at  $E_{\text{lab}} = 104$  [1,2], 139 [3], 172.5 [4] and 240 MeV [15] in comparison with the OM and CC results given by the complex folded OP. The elastic  $\alpha$  scattering on the Hoyle state is predicted by the OM calculation using the diagonal  $\alpha + {}^{12}\text{C}^*(0_2^+)$  folded OP with  $N_I$  chosen (see Table 1) to reproduce the measured inelastic  $\alpha + {}^{12}\text{C}^*(0_2^+)$  scattering cross section in the CC calculation.

To fine tune the strength of complex CDJLM interaction (5) which has been obtained in the nuclear matter limit (4), the optical model (OM) analysis of the measured elastic  $\alpha + {}^{12}\text{C}$  scattering data was done at each energy using the complex OP determined from the elastic folded potential (6) as

$$U_0(R) = N_R \text{Re}[U_{0_1^+ \rightarrow 0_1^+}(R)] + i N_I \text{Im}[U_{0_1^+ \rightarrow 0_1^+}(R)] + V_C(R), \quad (7)$$

where  $V_C(R)$  is the elastic Coulomb potential taken, for simplicity, as that between a point charge and a uniform charge distribution of radius  $R_C = 1.3 \times (4^{1/3} + 12^{1/3})$  fm. The renormalization coefficients  $N_R$  and  $N_I$  of the real and imaginary elastic folded potentials were adjusted first to the best OM fit of the elastic scattering data and then used further to scale the real and imaginary inelastic folded FF for the DWBA calculation, a standard method used so far in the folding + DWBA analyses of inelastic  $\alpha$ -nucleus scattering [15,17,25,26]. Since  $N_R$  and  $N_I$  are an approximate way to take into account the higher-order (dynamic polarization) contributions to the microscopic OP [25,34], they need to be readjusted again (to fit the elastic data) in the CC calculation, to account for the remaining nonelastic channels which were not included into the CC scheme. For consistency, these new  $N_R$  and  $N_I$  factors are also used to scale the complex inelastic folded FF for the CC calculation. The OM and CC descriptions of the elastic  $\alpha+^{12}\text{C}$  scattering at the considered energies are shown in Fig. 2 and the corresponding OP parameters are given in Table 1. One can see from Table 1 that the  $N_R$  coefficient given by the best OM fit of the elastic scattering data is slightly above unity which indicates that the new CDJLM interaction is quite a realistic choice for the double-folding calculation of the  $\alpha$ -nucleus potential. The best fit  $N_I$  of about 1.3 to 1.5 given by the OM calculation is not unexpected because the imaginary part of the CDJLM interaction is based on the BHF results for nuclear matter and gives, therefore, only a “volume” absorption. As a result, the imaginary folded OP cannot properly account for the surface absorption caused by inelastic scattering to the low-lying collective excitations and transfer reactions, and the OM fit to the elastic data naturally requires an enhanced  $N_I$  coefficient. The best-fit folded optical potentials give volume integrals  $J_{R(I)}$  and total reaction cross sections  $\sigma_R$  very close to those obtained earlier in the folding model analysis using a phenomenological imaginary OP [30] or in the model-independent Fourier-Bessel analyses of the elastic  $\alpha+^{12}\text{C}$  scattering data [33]. Thus, the elastic distorted waves given by the CDJLM folded OP should be quite accurate for the DWBA analysis of the inelastic  $\alpha+^{12}\text{C}$  scattering.

The DWBA results obtained with the complex folded OP and inelastic folded FF are compared with the measured cross section for inelastic  $\alpha+^{12}\text{C}$  scattering to the Hoyle state in Figs. 3 and 4. We found that the calculated DWBA cross sections systematically overestimate data at all energies if the inelastic folded FF is obtained with the (*unrenormalized*) RGM transition density [8]. Given the accurate choice of the density dependent  $NN$  interaction and nuclear densities, this discrepancy is clearly not associated with usual uncertainties of the folding model analysis of  $\alpha$ -nucleus scattering [26]. Since the RGM transition density has been proven to reproduce nicely the  $(e, e')$  data [8,12], the folding + DWBA results shown in Figs. 3 and 4 might indicate a “suppression” of the monopole  $E0$  strength occurred in the inelastic  $\alpha+^{12}\text{C}$  scattering. To further probe this effect, we have used a realistic Fermi distribution for the g.s. density of  $^{12}\text{C}$  [30] to generate the BM transition density (3)

Table 1

Renormalization coefficients  $N_{R(I)}$  of the complex folded OP and inelastic FF used in the DWBA and CC analyses of  $\alpha+^{12}\text{C}$  scattering at  $E_{\text{lab}} = 104, 139, 172.5,$  and  $240$  MeV.  $J_{R(I)}$  are volume integrals of the real and imaginary OP, and  $\sigma_R$  is the corresponding total reaction cross section.  $\text{CC}_{\text{en}}$  are the OP parameters in the entrance  $\alpha+^{12}\text{C}_{\text{g.s.}}$  channel of the CC calculation.  $\text{CC}_{\text{ex}}$  are those of the OP in the exit  $\alpha+^{12}\text{C}^*(0_2^+)$  channel, where  $N_I$  was adjusted to reproduce the inelastic  $0_2^+$  data using the original RGM transition density [8].

$E_{\text{lab}}$ (MeV)	Analysis	$N_R$	$J_R$ (MeV fm <sup>3</sup> )	$N_I$	$J_I$ (MeV fm <sup>3</sup> )	$\sigma_R$ (mb)
104	DWBA	0.975	312.3	1.295	104.3	799.5
	$\text{CC}_{\text{en}}$	1.015	325.1	1.066	81.76	794.1
	$\text{CC}_{\text{ex}}$	1.015	325.1	2.500	201.4	1349
139	DWBA	1.025	287.4	1.374	120.2	770.8
	$\text{CC}_{\text{en}}$	1.049	294.2	1.064	93.06	739.7
	$\text{CC}_{\text{ex}}$	1.049	294.2	2.500	218.6	1287
172.5	DWBA	1.156	285.4	1.506	117.5	736.7
	$\text{CC}_{\text{en}}$	1.165	287.6	1.264	98.64	716.9
	$\text{CC}_{\text{ex}}$	1.165	287.6	3.000	234.1	1288
240	DWBA	1.127	252.8	1.340	111.0	659.1
	$\text{CC}_{\text{en}}$	1.145	256.9	1.241	102.8	656.4
	$\text{CC}_{\text{ex}}$	1.145	256.9	3.400	281.6	899.1

for the DWBA analysis of inelastic scattering to the Hoyle state. We have fixed the monopole deformation parameter  $\beta$  so that (3) gives exactly the same  $E0$  transition strength as that given by the RGM transition density and, hence, exhausts 22.8% of the isoscalar monopole EWSR as discussed above. As can be seen from Figs. 3 and 4, the DWBA cross sections given by the inelastic FF folded with the BM transition density for the Hoyle state are very close to those given by the RGM transition density. To match the calculated DWBA cross section to the data points, we need to scale both transition densities by a factor of 0.55 which reduces the sum rule strength of the Hoyle state to  $S_0 \approx 6.9\%$  of the EWSR. Such a small sum rule strength is significantly below the empirical range of 15 - 20% of the EWSR discussed above. Given an accurate energy dependence of the CDJLM interaction, with its density dependence carefully calibrated against the BHF results at each energy, the RGM and BM transition densities scaled by the same factor of 0.55 give reasonable DWBA descriptions of the data at four considered energies. The sum rule strength of the Hoyle state found in our DWBA analysis is comparable to that ( $7.6 \pm 0.9\%$ ) found in the folding + DWBA analysis of the inelastic  $\alpha+^{12}\text{C}$  scattering at 240 MeV [15], where a Gaussian has been used for the



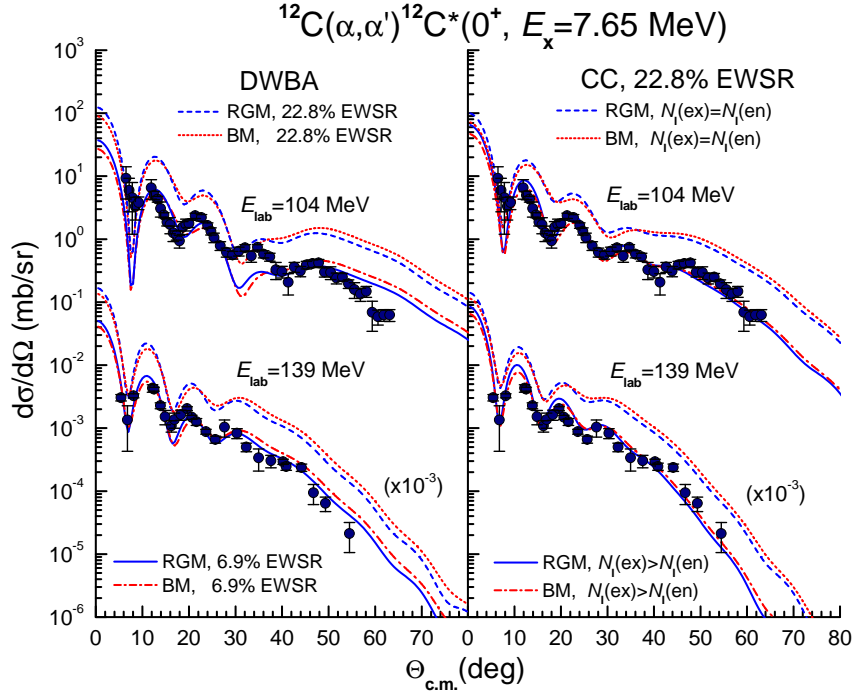


Fig. 3. Inelastic  $\alpha+^{12}\text{C}$  scattering data at  $E_{\text{lab}} = 104$  [1,2] and 139 [3] MeV for the  $0_2^+$  state of  $^{12}\text{C}$  in comparison with the DWBA and CC results given by the complex folded OP and inelastic FF obtained with two choices of the transition density for the  $0_2^+$  state. A good DWBA description of the data is reached only if the transition densities are scaled by a factor of 0.55 which reduces  $E0$  sum rule strength to  $S_0 \approx 6.9\%$  of the monopole EWSR. If  $S_0$  is kept at 22.8% of the EWSR, as given by the RGM result [8], the data can be reproduced in the CC calculation only by using a more absorbing OP for the  $\alpha+^{12}\text{C}^*(0_2^+)$  channel. See more details in text.

$\alpha N$  interaction in the folding calculation of the OP and inelastic FF.

A widely used prescription for the DWBA calculation of inelastic hadron scattering is to assume the same complex OP for the entrance and exit channels [16] and the only difference in the elastic waves is a slight shift in kinematics caused by a lower energy in the exit channel. For such a subtle nuclear state like the Hoyle state which has unusually dilute and extended structure [6], the diagonal potential  $U_{0_2^+ \rightarrow 0_2^+}$  should be quite different from  $U_{0_1^+ \rightarrow 0_1^+}$  which was used as the OP in both the entrance and exit channels of the DWBA calculation presented above. Actually, the importance of using explicitly different OP for different exit channels in the CC description of  $\alpha+^{12}\text{C}$  scattering at 104 and 139 MeV was pointed out earlier by Bauhoff [17]. Thus, one must go beyond DWBA and do the CC analysis of inelastic  $\alpha+^{12}\text{C}$  scattering to the Hoyle state before making any conclusion on the missing monopole strength. Although the  $E2$  transition between  $0_2^+$  and  $2_1^+$  states is quite weak and  $0_2^+$  state does *not* belong to a two-phonon ( $2_1^+ \otimes 2_1^+$ ) band, given the importance

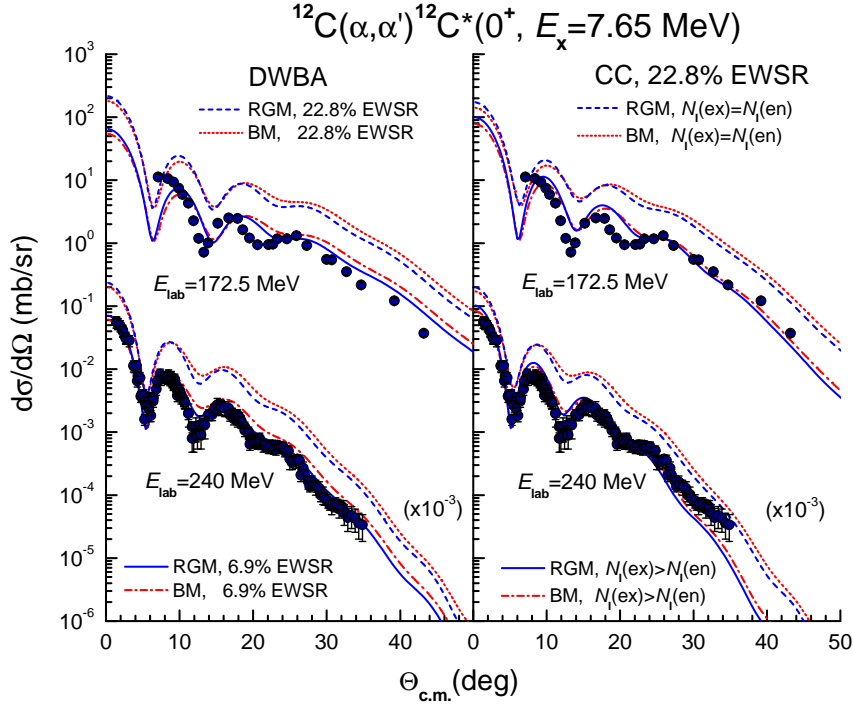


Fig. 4. The same as Fig. 3 but for the data measured at  $E_{\text{lab}} = 172.5$  [4] and 240 [15] MeV.

of  $0_2^+ \rightarrow 2_1^+$  transition in the stellar Carbon production, we have considered following coupling scheme in our CC calculation

$$0_1^+ \leftrightarrow 2_1^+ \leftrightarrow 0_2^+ \leftrightarrow 0_1^+. \quad (8)$$

In the CC scheme (8), the two-step excitation ( $0_1^+ \rightarrow 2_1^+ \rightarrow 0_2^+$ ) of the Hoyle state is treated in equal footing with the direct excitation ( $0_1^+ \rightarrow 0_2^+$ ). Thus, the CC description of the inelastic  $\alpha+^{12}\text{C}$  scattering to  $0_2^+$  state should be more realistic compared to the DWBA calculation which takes into account the direct excitation only [35]. For the inputs of the CC calculation, in addition to three inelastic FF's for transitions between  $0_1^+$ ,  $2_1^+$  and  $0_2^+$  states, three complex OP's have been calculated using the diagonal nuclear densities of these states given by the RGM calculation [8] and CDJLM interaction (5). For consistency, the  $N_{R(I)}$  factors have been readjusted again to obtain a good CC description of the elastic scattering data, as shown in Fig. 2. While the best-CC-fit  $N_R$  factor (see Table 1) remains more or less the same,  $N_I$  factor becomes significantly smaller and closer to unity, especially at the two low energies. This result shows explicitly how the inelastic channels in the CC scheme (8) contribute to the enhanced  $N_I$  factor found in the OM analysis of elastic scattering. With the increasing energy, more nonelastic channels are open and the best-CC-fit  $N_I$  factor remains around 1.2 to 1.3 at 172.5 and 240 MeV. All the CC results are shown in the right panels of Figs. 3

and 4, and it can be seen that the CC cross sections strongly overestimate the inelastic data for  $0_2^+$  state, in the same way as found in the DWBA calculation, when the inelastic FF is obtained with the original RGM transition density [8]. The two-step excitation ( $0_1^+ \rightarrow 2_1^+ \rightarrow 0_2^+$ ) was found to be negligible at all considered energies and the CC cross sections shown in Figs. 3 and 4 are practically given by the direct (one-step) excitation of  $0_2^+$  state only. We note that the original RGM density for the  $2_1^+ \rightarrow 0_2^+$  transition could not reproduce the observed  $B(E2)$  transition probability and we have scaled this transition density, as recommended in Ref. [8], by a factor of 1.53 to reproduce the experimental transition rate  $B(E2, 2_1^+ \rightarrow 0_2^+) \approx 2.6 \pm 0.8 e^2\text{fm}^4$  [36]. Despite such an enhancement, the folded  $2_1^+ \rightarrow 0_2^+$  transition FF gives still a very weak contribution to the CC cross section for the  $0_2^+$  excitation. An agreement with data can be reached only if the  $E0$  transition density is reduced by about half as found in the DWBA analysis. It is clear now that the missing monopole strength in the inelastic  $\alpha+^{12}\text{C}$  scattering to the Hoyle state is *not* associated with uncertainties of the DWBA or CC analyses, and there should be some physics effect that damps the  $E0$  transition strength. We further mention a recent folding + CC calculation of inelastic  $\alpha+^{12}\text{C}$  scattering at  $E_{\text{lab}} = 172.5, 240$  and  $386$  MeV (using the same RGM nuclear densities and DDM3Y interaction) by Takashina [37], where coupling to all the low-lying excited states of  $^{12}\text{C}$  as well as  $3\text{-}\alpha$  breakup channel was taken into account, but the CC cross section for the  $0_2^+$  excitation remains lying significantly higher than the data points, in about the same manner as found in our CC analysis.

Such a “damping” of the transition strength in inelastic nucleus-nucleus scattering has also been observed in our recent folding model study [38] of inelastic  $^{16}\text{O}+^{16}\text{O}$  scattering to the  $2_1^+$  and  $3_1^-$  states of  $^{16}\text{O}$ . Given the electric transition strengths of these states of  $^{16}\text{O}$  well determined from the  $(e, e')$  data (like the Hoyle state considered here), the DWBA or CC description of high-precision inelastic  $^{16}\text{O}+^{16}\text{O}$  scattering data, which cover a wide angular range and 6 orders of the cross-section magnitude, was possible only if the absorption in the exit channel is significantly increased [38]. Such an enhanced absorption was also found for the exit channel of one-neutron transfer  $\text{o}17\text{o}15$  reaction to the  $3/2^-$  excited state of  $^{15}\text{O}$  [39]. The enhanced absorption in the exit channel is a direct consequence of the suppression of nuclear refraction in nonelastic channels [29]. Namely, a short-lived (excited) and loosely bound cluster like  $^{16}\text{O}_{2^+}^*$  or  $^{15}\text{O}_{3/2^-}^*$  has a shorter mean free path in the nuclear medium which implies a weaker refraction or stronger absorption [40,41] in the exit channel compared to the entrance channel where both nuclei are in their (stable) ground states (for detailed discussion see Refs. [29,38,39]). In a similar scenario, the  $0_2^+$  state of  $^{12}\text{C}$  is very weakly bound and particle unstable (with a mean lifetime  $\tau \approx 10^{-16}$  s) and it is natural to expect that the OP in the  $\alpha+^{12}\text{C}^*(0_2^+)$  exit channel is more absorbing than the OP in the entrance  $\alpha+^{12}\text{C}$  channel. Since the elastic  $\alpha$  scattering on the Hoyle state cannot be

measured, we have adjusted the renormalization factor  $N_I$  of the imaginary OP of the  $\alpha+^{12}\text{C}^*(0_2^+)$  channel to achieve a reasonable CC description of the inelastic data for  $0_2^+$  state, while keeping  $N_R$  factor and complex strength of the transition FF unchanged. From Figs. 3 and 4 one can see that a very good CC description of the inelastic  $0_2^+$  data can be reached by using  $N_I \approx 2.5 - 3.4$  for the imaginary OP in the  $\alpha+^{12}\text{C}^*(0_2^+)$  channel (see Table 1). Such a strong absorptive OP predicts a very different elastic  $\alpha+^{12}\text{C}^*(0_2^+)$  scattering cross section compared to the measured elastic  $\alpha+^{12}\text{C}_{\text{g.s.}}$  scattering (see Fig. 2).

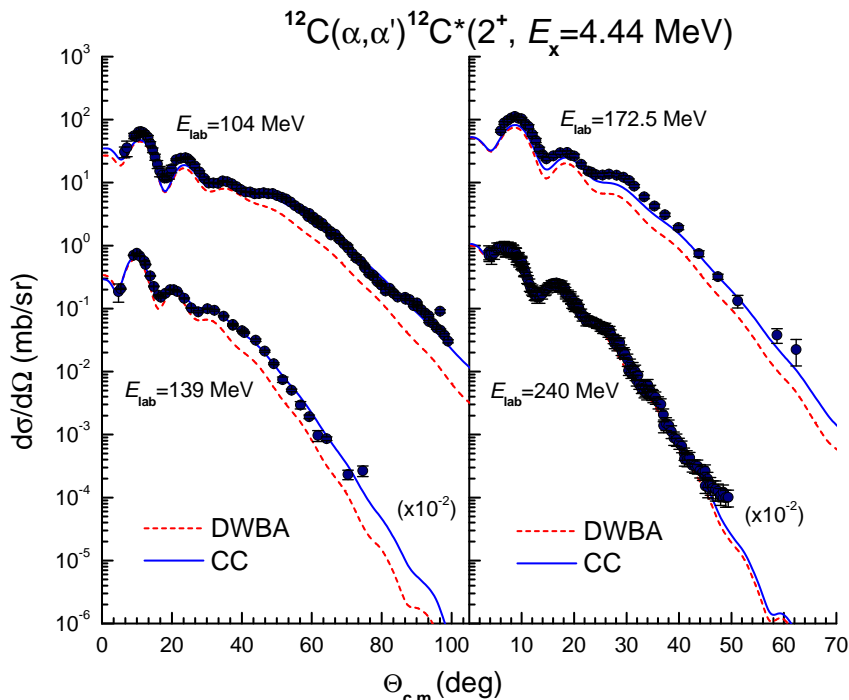


Fig. 5. Inelastic  $\alpha+^{12}\text{C}$  scattering data measured at  $E_{\text{lab}} = 104$  [1,2], 139 [3], 172.5 [4] and 240 [15] MeV for the  $2_1^+$  excitation at 4.44 MeV in  $^{12}\text{C}$  in comparison with the DWBA and CC results obtained with the complex folded OP and inelastic folded FF. See more details in text.

To illustrate whether the enhanced absorption is also required for some other excited states of  $^{12}\text{C}$  or is it a unique effect associated with fragile structure of the Hoyle state, we have done the same folding + DWBA (CC) analyses of inelastic  $\alpha+^{12}\text{C}$  scattering to the  $2_1^+$  state at 4.44 MeV using the RGM density and the results are plotted in Fig. 5. Like the Hoyle state, the RGM transition density of the  $2_1^+$  state has also been used to successfully reproduce the  $(e, e')$  data [8]. The electric transition strength predicted by the RGM transition density is  $B(E2, 0_1^+ \rightarrow 2_1^+) = 46.5 e^2\text{fm}^4$  which agrees fairly with the measured  $B(E2)$  transition rate of  $40 \pm 4 e^2\text{fm}^4$  [36,42]. We note that  $2_1^+$  state is a very strong excitation and the measured inelastic cross section becomes even comparable to the elastic scattering cross section at the medium angles where the nuclear scattering dominates (see Figs. 2 and 5). That is the reason why the coupling strength by the  $2_1^+$  excitation is strongest in our CC

scheme (8). From Fig. 5 one can see that a consistent folding model description of the inelastic  $\alpha+^{12}\text{C}$  scattering to the  $2_1^+$  state at  $\alpha$ -energy up to 172.5 MeV can be reached only in the CC calculation. If one stays within the DWBA framework, using the same inelastic folded FF, then the total strength of the  $E2$  transition density needs to be enlarged to reproduce the  $2_1^+$  data, but this would lead to a larger discrepancy between the calculated and experimental  $B(E2, 0_1^+ \rightarrow 2_1^+)$  values. It can also be seen from Table 1 that the coupling strength by the  $2_1^+$  excitation exhausts nearly all the surface enhancement of the imaginary OP at 104 and 139 MeV, and the best-CC-fit  $N_1$  factor is around unity compared to that of about 1.3 - 1.4 as given by the OM analysis. Finally, the measured inelastic  $\alpha+^{12}\text{C}$  scattering cross section for the  $2_1^+$  state is nicely reproduced by the CC calculation at all energies without the need to enhance the imaginary OP in the  $\alpha+^{12}\text{C}^*(2_1^+)$  channel, i.e.,  $\text{CC}_{\text{en}}$  set of the  $N_{\text{R(I)}}$  factors in Table 1 was also used for the exit  $\alpha+^{12}\text{C}^*(2_1^+)$  channel. This indicates that the enhanced absorption found above for the  $\alpha+^{12}\text{C}^*(0_2^+)$  channel seems to be associated particularly with the fragile structure and short lifetime of the Hoyle state. We recall that the  $2_1^+$  state of  $^{12}\text{C}$  is more robust and particle stable, and it decays via  $\gamma$ -emission only. With a mean lifetime  $\tau \approx 6 \times 10^{-14}$  s [42] the  $2_1^+$  state lives about 600 times longer than the Hoyle state and 10 times longer than the  $2_1^+$  state of  $^{16}\text{O}$  for which the absorption enhancement has been found in the folding model study of inelastic  $^{16}\text{O}+^{16}\text{O}$  scattering [38]. Although our folding model analysis was done using a new complex density dependent interaction, the absorption enhancement found for the exit  $\alpha+^{12}\text{C}^*(0_2^+)$  channel is not a feature associated with the new interaction. In fact, such a large absorption has already been established in the semi-microscopic CC analysis of the same  $\alpha+^{12}\text{C}$  data by Ohkubo and Hirabayashi [19]. These authors have used phenomenological Woods-Saxon (WS) potentials of the same geometry for the imaginary OP in all exit channels of the inelastic  $\alpha+^{12}\text{C}$  scattering and adjusted the WS depth each case to reproduce the inelastic data. From Table I of Ref. [19] one can find that the WS imaginary OP for the  $\alpha+^{12}\text{C}^*(0_2^+)$  channel is nearly 4 times deeper than that for the entrance  $\alpha+^{12}\text{C}_{\text{g.s.}}$  channel, while the best-fit WS depth found for the  $\alpha+^{12}\text{C}^*(2_1^+)$  channel is only slightly larger than that of the  $\alpha+^{12}\text{C}_{\text{g.s.}}$  channel. For the  $3_1^-$  state of  $^{12}\text{C}$  the CC calculation of Ref. [19] has shown also a sizable enhancement of absorption, in an agreement with the results of our CC analysis using the CDJLM interaction which will be presented elsewhere. We note further that small fraction ( $S_0 \approx 9\%$ ) of the monopole EWSR found in the DWBA analyses of inelastic  $^3\text{He}, ^6\text{Li}+^{12}\text{C}$  scattering to the Hoyle state [13,14] could well be associated with the same absorption effect as that found in the present work.

Our results of the CC description of inelastic  $\alpha+^{12}\text{C}$  scattering to the Hoyle state as well as those of inelastic scattering and one-neutron transfer reaction measured with the  $^{16}\text{O}+^{16}\text{O}$  system [38,39] show clearly that there is a correlation between the weak binding and/or short lifetime of the *excited*

target-like cluster and the *absorption* in the exit channel of a quasi-elastic scattering reaction. Although it is still difficult to establish a systematic for this “absorption” phenomenon, the results obtained so far indicate the need to have a realistic choice for the OP not only in the entrance but also in the exit channel of the inelastic nucleus-nucleus scattering. The standard method of choosing the same complex OP in both the entrance and exit channels of nucleus-nucleus scattering might lead to a large uncertainty in the deduced transition strength if one simply scales the inelastic FF to match the DWBA or CC results to the measured angular distributions. In particular, this effect must be accurately taken into account in the study of the nucleus-nucleus scattering measured with unstable beams where nuclei in the entrance and exit channels are very differently bound.

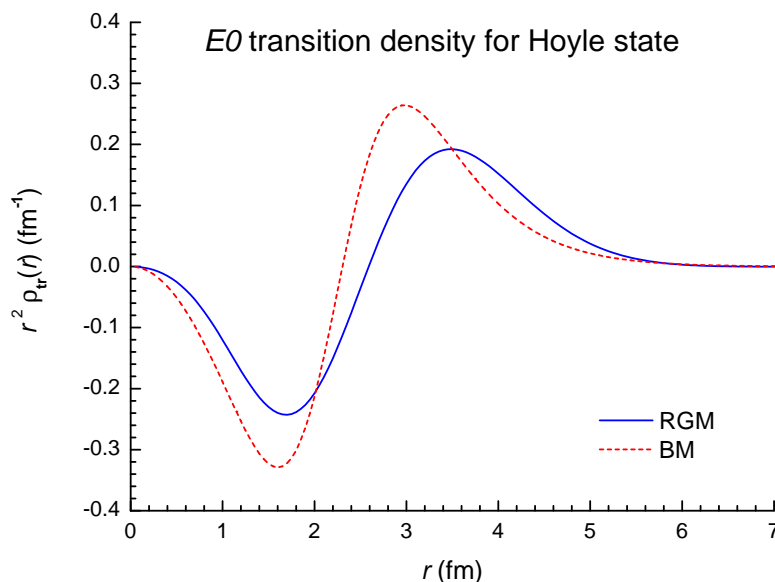


Fig. 6.  $0_1^+ \rightarrow 0_2^+$  transition densities for the Hoyle state given by the RGM calculation of Kamimura [8] and BM model (3). The deformation parameter  $\beta$  of the BM density was adjusted to reproduce the same monopole transition strength as that given by the RGM transition density which exhausts 22.8% of the isoscalar monopole EWSR.

We discuss now briefly the choice for the  $E0$  transition density of the Hoyle state. It is a common belief that the breathing mode (BM) model (3) is more appropriate for the transition density of a giant monopole resonance (in medium and heavy nuclei) that exhausts a large fraction of the monopole EWSR [23]. Although the BM density was scaled to reproduce the monopole transition moment given by the RGM density [8] before being used in our folding calculation, its radial dependence (see Fig. 6) should not contain any feature of the  $\alpha$  cluster or BEC structure of the Hoyle state. Therefore, it is quite surprising to see that the BM transition density gives nearly the same DWBA and CC descriptions of the inelastic  $0_2^+$  data as those given by the  $3\text{-}\alpha$

RGM transition density (see Figs. 3 and 4). One can see in Fig. 6 that the two densities have the same asymptotic tail at  $r > 6$  fm while the node and two extrema of the BM density are shifted inward to smaller radii compared to the RGM density. However, as shown in Figs. 3 and 4, such a difference in the two densities gives only a minor difference in the calculated inelastic scattering cross sections. Consequently, the success of the BEC or RGM nuclear densities in the CC description of inelastic  $\alpha+^{12}\text{C}$  scattering to the  $0_2^+$  state reported so far [18,19,20,21] is an important evidence, but *not* the unambiguous proof for the  $\alpha$ -condensate structure of the Hoyle state. In fact, a closer inspection of the structure models by Chernykh *et al.* [11] has revealed that the structure of the Hoyle state could be somewhat more complicated than just a condensate of three  $\alpha$  particles.

In conclusion, a realistic (complex) density dependence was introduced into the M3Y-Paris interaction, based on the Brueckner Hartree Fock calculation of nuclear matter, for the folding model study of the  $\alpha+^{12}\text{C}$  scattering at  $E_{\text{lab}} = 104$  to 240 MeV. Given an accurate estimation of the bare  $\alpha+^{12}\text{C}$  optical potential, our folding model analysis has shown consistently that there should be an enhancement of absorption in the exit  $\alpha+^{12}\text{C}^*(0_2^+)$  channel due to the short lifetime and weakly bound structure of the Hoyle state, which accounts for the “missing” monopole strength of the Hoyle state observed earlier in the DWBA analysis of inelastic  $\alpha+^{12}\text{C}$  scattering.

## Acknowledgments

The authors are grateful to Prof. W. von Oertzen, Prof. S. Ohkubo, Dr. M. Takashina and Dr. X. Chen for their helpful communications. We also thank Prof. M. Kamimura for providing us with the revised parametrization of the RGM densities from Ref. [8].

## References

- [1] G. Hauser, R. Löhken, H. Rebel, G. Schatz, G.W. Schweimer, and J. Specht, Nucl. Phys. A 128 (1969) 81.
- [2] J. Specht, G.W. Schweimer, H. Rebel, G. Schatz, R. Löhken, G. Hauser, Nucl. Phys. A 171 (1971) 65.
- [3] S.M. Smith, G. Tibell, A.A. Cowley, D.A. Goldberg, H.G. Pugh, W. Reichart, N.S. Wall, Nucl. Phys. A 207 (1973) 273.

- [4] S. Wiktor, C. Mayer-Böricke, A. Kiss, M. Rogge, P. Turek, and H. Dabrowski, *Acta Phys. Pol. B* 12 (1981) 491; A. Kiss, C. Mayer-Böricke, M. Rogge, P. Turek, and S. Wiktor, *J. Phys. G* 13 (1987) 1067.
- [5] P. Strehl, *Z. Phys.* 234 (1970) 416.
- [6] M. Freer, *J. Phys. G* 34 (2007) 789; M. Freer, to appear in *Proceedings of Intern. Symp. on Physics of Unstable Nuclei (ISPUN07)* (World Scientific: Singapore).
- [7] E. Uegaki, S. Okabe, Y. Abe, H. Tanaka, *Prog. Theor. Phys.* 57 (1977) 1262.
- [8] M. Kamimura, *Nucl. Phys. A* 351 (1981) 456; M. Kamimura, private communication.
- [9] A. Tohsaki, H. Horiuchi, P. Schuck, G. Röpke, *Phys. Rev. Lett.* 87 (2001) 192501.
- [10] Y. Funaki, A. Tohsaki, H. Horiuchi, P. Schuck, G. Röpke, *Phys. Rev. C* 67 (2003) 051306(R).
- [11] M. Chernykh, H. Feldmeier, T. Neff, P. von Neumann-Cosel, A. Richter, *Phys. Rev. Lett.* 98 (2007) 032501.
- [12] Y. Funaki, A. Tohsaki, H. Horiuchi, P. Schuck, G. Röpke, *Eur. Phys. J. A* 28 (2006) 259.
- [13] D. Lebrun, M. Buenerd, P. Martin, P. de Saintignon, G. Perrin, *Phys. Lett.* 97 B (1980) 358.
- [14] W. Eyrich, A. Hofmann, A. Lehmann, B. Mühldorfer, H. Schlösser, H. Wirth, H. J. Gils, H. Rebel, S. Zagromski, *Phys. Rev. C* 36 (1987) 416.
- [15] B. John, Y. Tokimoto, Y.W. Lui, H.L. Clark, X. Chen, D.H. Youngblood, *Phys. Rev. C* 68 (2003) 014305.
- [16] G.R. Satchler, *Direct Nuclear Reactions* (Clarendon Press: Oxford, 1983).
- [17] W. Bauhoff, *Phys. Lett.* 139 B (1984) 223.
- [18] Y. Hirabayashi, S. Ohkubo, *Phys. At. Nuclei* 65 (2002) 683.
- [19] S. Ohkubo, Y. Hirabayashi, *Phys. Rev. C* 70 (2004) 041602(R).
- [20] M. Takashina, Y. Sakuragi, *Phys. Rev. C* 74 (2006) 054606.
- [21] S. Ohkubo, Y. Hirabayashi, *Phys. Rev. C* 75 (2007) 044609.
- [22] A.M. Kobos, B.A. Brown, P.E. Hodgson, G.R. Satchler, A. Budzanowski, *Nucl. Phys. A* 384 (1982) 65.
- [23] D.J. Horen, J.R. Beene, G.R. Satchler, *Phys. Rev. C* 52 (1995) 1554.
- [24] D.T. Khoa, G.R. Satchler, W. von Oertzen, *Phys. Rev. C* 56 (1997) 954.
- [25] D.T. Khoa, G.R. Satchler, *Nucl. Phys. A* 668 (2000) 3.



- [26] G.R. Satchler, D.T. Khoa, Phys. Rev. C 55 (1997) 285.
- [27] J.P. Jeukenne, A. Lejeune, C. Mahaux, Phys. Rev. C 16 (1977) 80.
- [28] N. Anantaraman, H. Toki, and G.F. Bertsch, Nucl. Phys. A 398 (1983) 269.
- [29] D.T. Khoa, W. von Oertzen, H.G. Bohlen, S. Ohkubo, J. Phys. G 34 (2007) R111.
- [30] D.T. Khoa, Phys. Rev. C 63 (2001) 034007.
- [31] D.K. Srivastava, H. Rebel, J. Phys. G 10 (1984) L127.
- [32] J. Raynal, Computing as a Language of Physics (IAEA, Vienna, 1972) p.75; J. Raynal, coupled-channel code ECIS97 (unpublished).
- [33] C.J. Batty, E. Friedman, H.J. Gils, H. Rebel, Adv. Nucl. Phys. 19 (1989) 1.
- [34] H. Feshbach, *Theoretical Nuclear Physics* Volume II (Wiley-Interscience: New York, 1992).
- [35] W. von Oertzen, private communication.
- [36] P.M. Endt, At. Data and Nucl. Data Tables 23 (1979) 3; F. Ajenberg-Selove, Nucl. Phys. A 506 (1990) 1.
- [37] M. Takashina, talk presented at DREB07 Workshop, June 2007.
- [38] D.T. Khoa, H.G. Bohlen, W. von Oertzen, G. Bartnitzky, A. Blazevic, F. Nuoffer, B. Gebauer, W. Mittig, P. Roussel-Chomaz, Nucl. Phys. A 759 (2005) 3.
- [39] H.G. Bohlen, D.T. Khoa, W. von Oertzen, B. Gebauer, F. Nuoffer, G. Bartnitzky, A. Blazevic, W. Mittig, P. Roussel-Chomaz, Nucl. Phys. A 703 (2002) 573.
- [40] J.P. Jeukenne, A. Lejeune, C. Mahaux, Phys. Rep. 25 (1976) 83; Phys. Rev. C 16 (1977) 80.
- [41] J.W. Negele, K. Yazaki, Phys. Rev. Lett. 47 (1981) 71.
- [42] S. Raman, C.W. Nestor Jr., P. Tikkanen, At. Data and Nucl. Data Tables 78 (2001) 1.